Supporting Information for the manuscript: ***Expanding the rule set of DNA circuitry with associative toehold activation***, by Xi Chen.

Content: **Text S1** to **S3**; **Figure S1** to **S6**.

Text S1: Procedures of data acquisition and processing

The excitation/emission wavelengths for the fluorescent reporters were 495/520 nm for FAM and 641/663 nm for TYE665. The relative fluorescence units (RFUs) reported in **Figures 2**, **3**, **4**, and **6** were the values directly given by the plate-reader. Note that the scale of RFUs between different fluorophores cannot be directly compared as they are affected by the brightness of the dyes, purity of the dye-containing oligonucleotides (which affects quenching efficiency), as well as various wavelength-dependent optic and electronic factors of the plate reader.

The procedures below were followed to obtain the concentration of a target molecule (typically the end-product of a DNA circuit):

First, the RFU of the quenched fluorescent reporter alone was noted as RFU_ZERO.

Second, a reaction was set up where the one precursor of the final product (of known concentration) was the limiting reactant. Sufficient catalyst and other reactants were added to the reaction, which was allowed to reach near completion. The RFU-vs-time plot was then fitted to a single-exponential or double-exponential equation from which the asymptotic RFU as time approaches infinite was calculated and noted as RFU_FULL. Thus, the RFU_FULL corresponds to the RFU value when all of the limiting reactant is converted into the product.

Third, the product concentration at any given time point was calculated by interpolating the RFU value at this time point between RFU_ZERO and RFU_FULL. Equivalently, a new scale of product concentration was linearly drawn between RFU_ZERO and RFU_FULL on the right side of each kinetic trace. The linearity between product concentration and fluorescent signal had been experimentally verified.

For single-turnover reactions shown in **Figure 2b** and **2c**, all RFU-vs-time plots were approximately fitted into a single-exponential equation (the approximation was valid since the concentration of the invader strand was in large excess) from which the pseudo-first-order rate constants k could be obtained. The k values were then divided by the concentration of the invader strand (in this case 25 nM) to obtain the apparent second order rate constant k_{app}.

Text S2: Structure of DNA 3-way junctions

To better envision the mechanism of strand displacement across a 3-way junction, it is worthwhile to discuss the structures of DNA 3-way junctions and their dependence on the DNA sequence around the junction. Standard terminology[1] is used in this discussion. Briefly, the 3-way junction is form by three strands named 1, 2, and 3 (**Figure S6**). In the 3-way junction, strand 2 contains two consecutive bulged bases, whereas strand 1 and 3 do not have any unpaired base. The 5' portion of strand 1 hybridizes to the 3' portion of strand 3, forming stem A. The 3' portion of strand 1 hybridizes to the 5' portion of strand 2, forming stem B. The 3' portion of strand 2 and the 5' portion of strand 3 form stem C.

In such a 3-way junction, there are two potential co-axial stacking options: A/C stack and A/B stack. B/C stack is energetically unfavorable. As suggested by a series of studies on the structure of 3-way junctions[1-2], the choice between A/B and A/C stacking is governed by the sequence near the junction. In particular, the sequence motifs shown in the insets of **Figure S6b** and **S6c** favor the formation of A/C stack and A/B stack, respectively.

Because both sequence motifs are based on the stable CTTG tetraloop and require a pyrimidine at a specific position near the junction, I collectively term these motifs CTTG/Y motifs. The representative NMR structures of A/C stack and A/B stack dictated by the two CTTG/Y motifs are shown in **Figure S6b** and **S6c**, respectively. The sequences of the 3-way junctions used in this study actually conform to the constraints of CTTG/Y motifs. It should be noted that although the CTTG/Y motif was chosen in this study, I expect there are many more sequences that stabilize 3-way junctions.[3]

Text S3: Discussion on rate constants of strand displacement across three-way junctions

To gain a more predictive understanding of the kinetics of strand displacement across a 3-way junction with bulged thymidines, the process shown in **Figure 1d** can be treated with a coarse-grained model, in which strand displacement after toehold binding is considered as one step with a pseudo-first order rate constant k_2. The second-order rate constant for toehold association and first-order rate constant for toehold dissociation are denoted as k_1 and k_{-1}, respectively. As suggested by Zhang and Winfree[4], under the experimental conditions used in this study, the concentrations of reactants ([$\mathbf{C2_x}$] = 25 nM, [**D:P**] = 10 nM) were low enough so that the rate of strand displacement was approximately proportional to [$\mathbf{C2_x}$] × [**D:P**], with the apparent second order rate constant $k_{app} = k_1k_2 / (k_{-1} + k_2)$. Moreover, for $\mathbf{C2_8}$, the toehold binding is sufficiently reversible (i.e. $k_{-1} >> k_2$), so that k_{app} is roughly k_1k_2 / k_{-1}, or k_2 / K_d, where $K_d = k_{-1} / k_1$ is the dissociation constant of toehold interaction. Since the K_d and k_{app} values for $\mathbf{C2_8}$ were predicted to be 40 μM and measured to be 3×10^3 /M/s, respectively, k_2 was estimated to be on the order of 0.1 s^{-1}, which is roughly 10-fold lower than that of conventional strand displacement (c.a. 1 s^{-1})[4] but much faster than remote toehold-mediated strand displacement (typically 0.005 to 0.02 s^{-1})[5]. Assuming the second order rate constant of toehold-independent strand displacement to be 1 /M/s[4-5], this estimated rate constant suggests that the 3-way junction with two bulged thymidines places the first base of the BM domain close to the 5' end of strand **P** with an effective local concentration of 0.1 M.

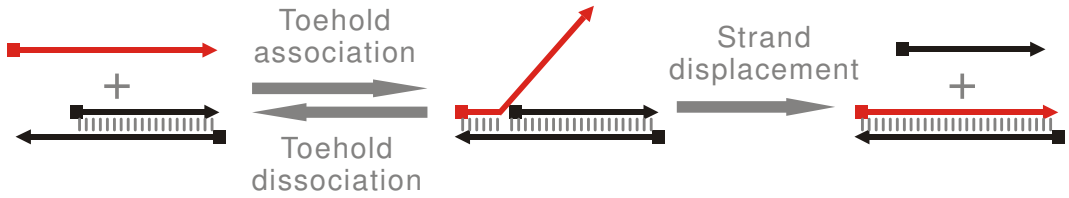

Figure S1. Scheme of toehold-mediated strand displacement.

Figure S2. Sequences of oligonucleotides used in the study of single-turnover strand displacement across a 3-way junction. The color-coding is the same as that used in **Figure 2**. Among these oligonucleotides, **F** and **Q** were ordered in HPLC-purified grade, **D** and **P** were ordered in desalted grade and PAGE-purified in-house, and the rest were ordered in desalted grade and used directly.

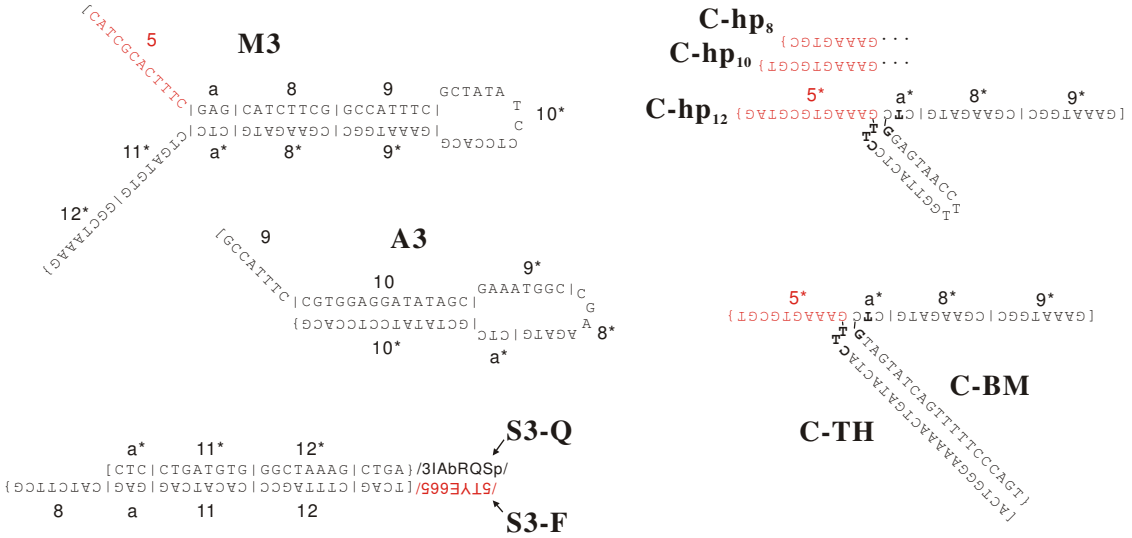

Figure S3. Sequences of oligonucleotides used in the study of multiple-turnover reactions. The color-coding is the same as that used in **Figure 3** and **4**. Among these oligonucleotides, **S3-F** and **S3-Q** were ordered in HPLC-purified grade, **M3** and **A3** were ordered in desalted grade and PAGE-purified in-house, and the rest were ordered in desalted grade and used directly.

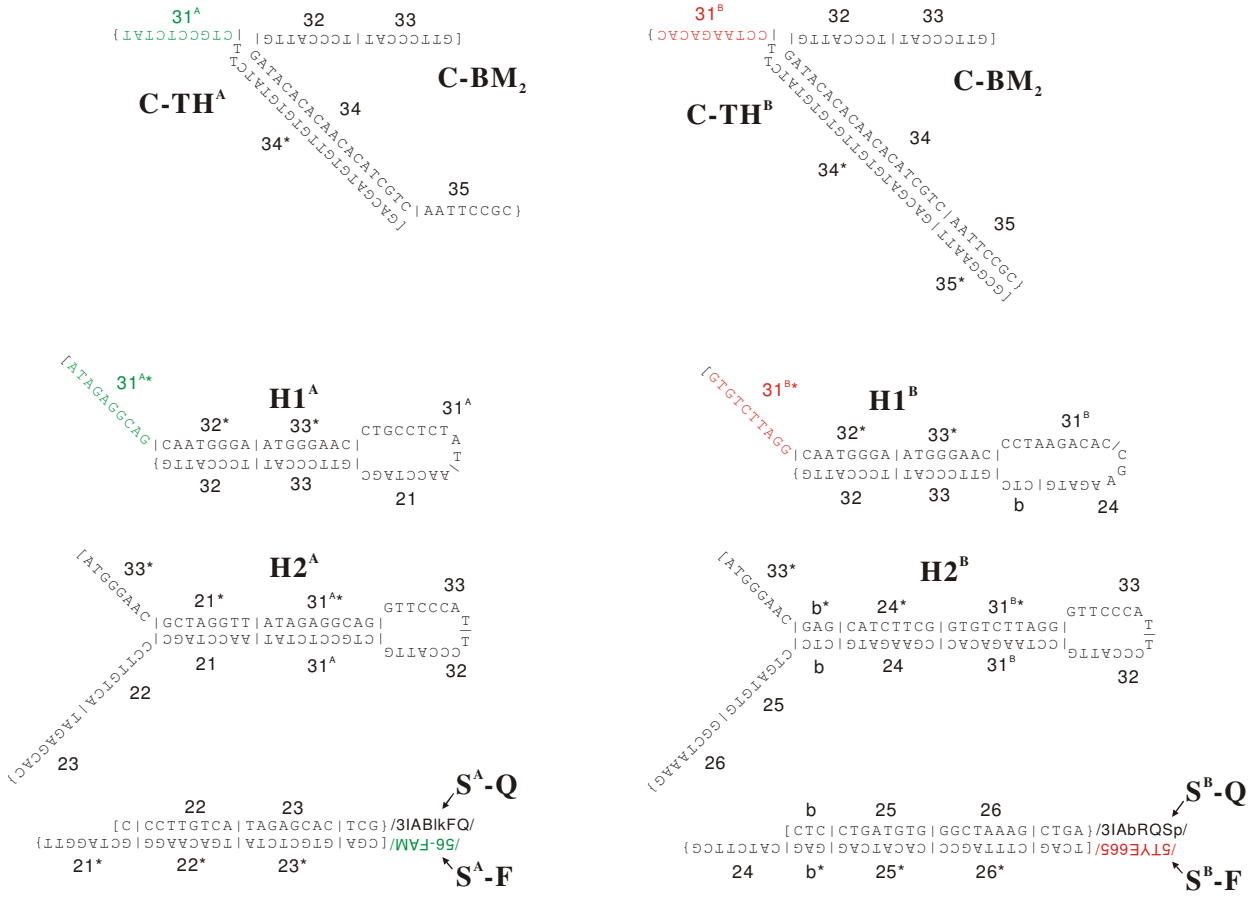

Figure S4. Sequences of oligonucleotides used in the study of toehold switching. The color-coding is the same as that used in **Figure 5**. Among these oligonucleotides, **S^{A}-Q**, **S^{B}-F**, and **S^{B}-Q** were ordered in HPLC-purified grade, **H1^{A}**, **H2^{A}**, **H1^{B}**, and **H2^{B}** were ordered in desalted grade and PAGE-purified in-house, and the rest were ordered in desalted grade and used directly.

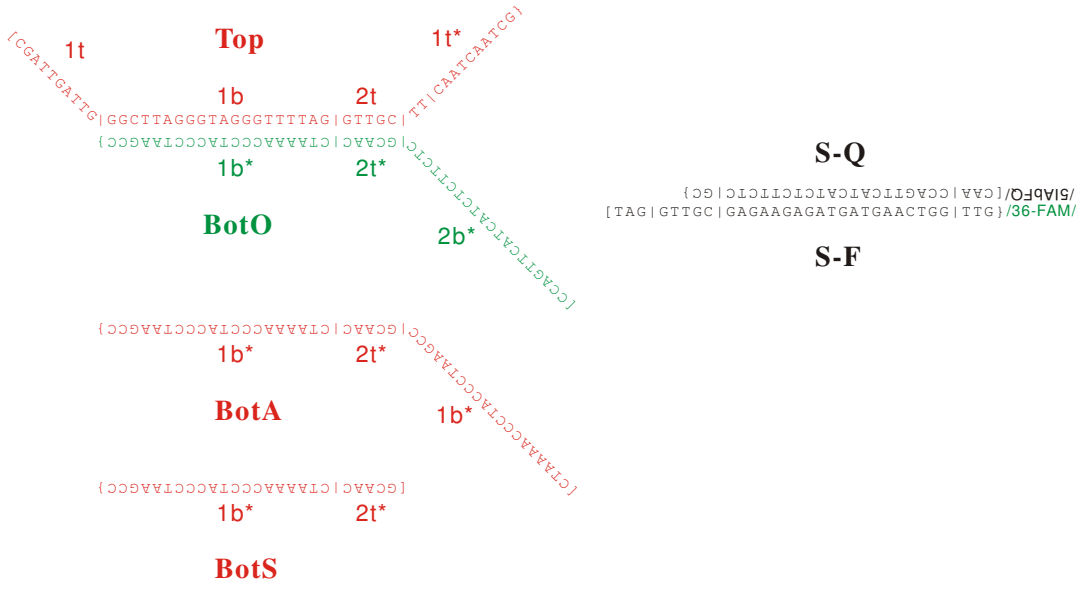

Figure S5. Sequences of DNA oligonucleotides used in the study of conformational self-replicator. The color-coding is the same as that used in **Figure 6**. Among these oligonucleotides, **S-Q** was ordered in HPLC-purified grade, **Top**, **BotO**, **BotA**, and **BotS** were ordered in desalted grade and PAGE-purified in-house, **S-F** was ordered in desalted grade and used directly.

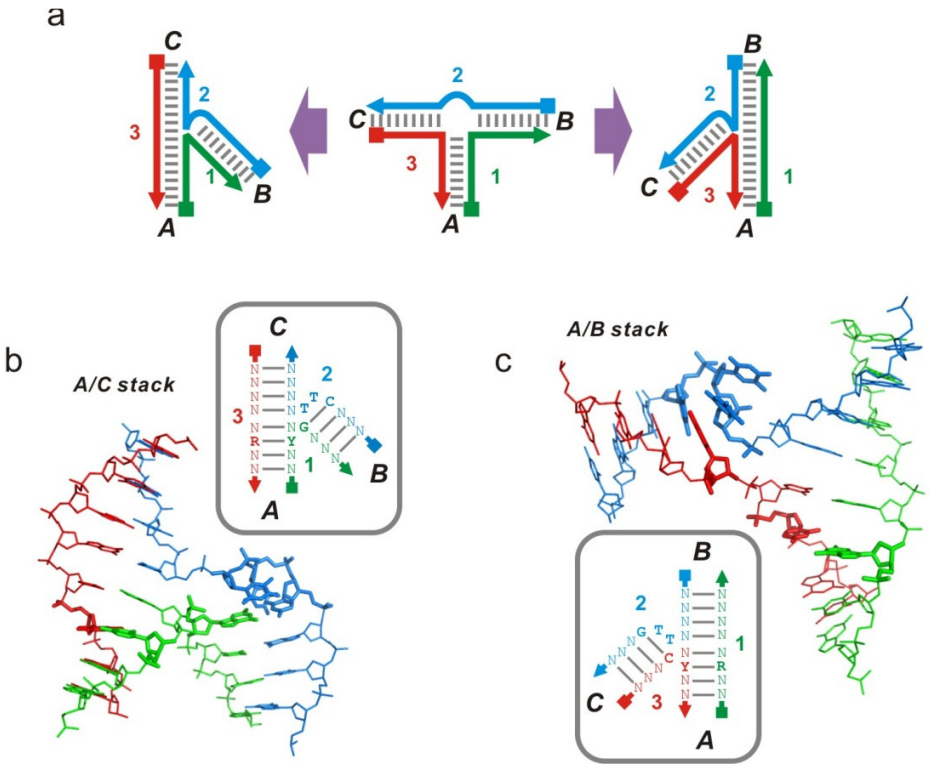

Figure S6. Two small structural motifs that stabilize DNA 3-way junction. (a) The terminology to describe the structure of a 3-way junction with bulged bases on one strand. Schematic presentation of A/C stack and A/B stack are shown on the left and right, respectively. (b and c) Representative NMR structures of the two conformations: A/C stack (a) and A/B stack (b), directed by the two sequence motifs around the 3-way junction (insets). The NMR structures shown in (b) and (c) are based on the first frame of PDB entries 1SNJ[1] and 1EZN[2], respectively.

References

(1) Wu, B.; Girard, F.; van Buuren, B.; Schleucher, J.; Tessari, M.; Wijmenga, S. *Nucleic Acids Res* **2004**, *32*, 3228.

(2) van Buuren, B. N.; Overmars, F. J.; Ippel, J. H.; Altona, C.; Wijmenga, S. S. *J Mol Biol* **2000**, *304*, 371.

(3) Altona, C. *J Mol Biol* **1996**, *263*, 568.

(4) Zhang, D. Y.; Winfree, E. *J Am Chem Soc* **2009**, *131*, 17303.

(5) Genot, A. J.; Zhang, D. Y.; Bath, J.; Turberfield, A. J. *J Am Chem Soc* **2011**, *133*, 2177.